Electronic Supplementary Material (ESI) for Lab on a Chip

Supporting Information

Modular Microfluidic System Fabricated in Thermoplastics for the Strain-Specific Detection of Bacterial Pathogens

Hui-Wen Chen,[1] Hong Wang,[1] Mateusz Hupert,[2] Makgorzata Witek,[2] Udara Dharmasiri,[1] Maneesh R. Pingle,[3] Francis Barany[3] and Steven A. Soper[2,4,5]

[1]Department of Chemistry
Louisiana State University
Baton Rouge, LA 70803

[2]Department of Biomedical Engineering
University of North Carolina, Chapel Hill
Chapel Hill, NC 27599

[3]Weill Cornell Medical College
New York, NY

[4]Department of Chemistry
University of North Carolina, Chapel Hill
Chapel Hill, NC 27599

[5]Nano-bioscience and Chemical Engineering, Ulsan National Institute of Science and Technology, Ulsan, South Korea

*Author to Whom Correspondence should be addressed: Steven A. Soper

Experimental Section

Materials and reagents. PC and PMMA sheets were purchased from Good Fellow (Berwyn, PA). Chemicals used for the PMMA surface modification and hybridization assays included 1-ethyl-3-(3-dimethylaminopropyl) carbodiimide hydrochloride (EDC), *N*-hydroxysuccinimide (NHS), and 20x SSC buffer (3 M sodium chloride, 0.3 M sodium citrate, pH 7.0), which were purchased from Sigma-Aldrich (St. Louis, MO). A 10% sodium dodecyl sulfate (SDS) stock solution, which was used for post-hybridization washing, was received from Ambion (Austin, TX). Polyethylene glycol (PEG, Mw = 8,000), sodium chloride (NaCl), ethanol, disodium hydrogen phosphate (Na_2HPO_4), sodium phosphate (Na_3PO_4), and 2-propanol were obtained from Sigma-Aldrich (St. Louis, MO). Oligonucleotide primers and probes were secured from Integrated DNA Technologies (Coralville, IA). Their sequences and melting temperatures (T_m) are listed in Table S1. *E. coli* K12 was obtained from American Type Culture Collection (Manassas, VA). Both *E. coli* O157:H7 and *Salmonella* cells were purchased from Kirkegaard & Perry Laboratories (Gaithersburg, MD). All solutions were prepared in nuclease free water purchased from Invitrogen Corporation (Carlsbad, CA).

Microfluidic cartridge fabrication. The PC motherboard contained a network of microchannels for cell lysis, SPE, PCR and LDR on the front-side of the substrate and thermal isolation grooves[1] and fluidic interconnects for the modules on the back-side, all of which were replicated in one-step using double-sided hot embossing from two brass molding tools mounted opposite to each other on a JENOPTIK HEX02 hot embossing machine (Jena, Germany). The brass mold masters were fabricated by high-precision micromilling as described elsewhere.[2] After hot embossing, the SPE bed contained 50 µm diameter micropillars spaced by 100 µm (center-to-center). The SPE bed on the PC motherboard as well as the corresponding area on the PC cover plate were exposed to 254 nm UV radiation (15 mW/cm^2) through a mask for 20 min to photo-oxidize the PC surface to allow for the solid-phase extraction of DNA from a whole cell lysate.[3] The PC motherboard was assembled to a PC cover plate (250 µm thick) using thermal fusion bonding at 150°C for 20 min.

The waveguide, universal array PMMA module consisted of a microchannel network for the DNA microarray on the front-side and the back-side was comprised of a planar air-embedded waveguide with integrated coupling prism.[4] This PMMA module was replicated by double-sided hot embossing from two brass molding tools. Twenty-four (4 x 6) waveguide modules could be fabricated on one PMMA wafer in a single replication step. Following spotting of the DNA probes onto the waveguide, the PMMA module was assembled by thermal fusion bonding the substrate to a PMMA cover plate at 107°C for 20 min.

PMMA cell enrichment module. The cell enrichment module was fabricated in PMMA using micro-replication via hot embossing, which has been reported previously.[5-7] Figure S1A-B depicts the topographical layout of the PMMA cell enrichment module.[8] The module contained 9.5 mm long, 16 curvilinear channels that were 15 µm in width and 80 µm in depth with a radius of curvature of 120 µm. The surface area of the 16 channels, which defined the cell selection bed, was 40 mm^2 with a volume of 250 nL. The width of each cell selection channel was chosen to maximize cell recovery by closely matching the selection channel width to the cell diameter.[9] While *E. coli* cells are oblate particles with dimensions on the order of 0.5 µm x 2 µm (short axis x long axis), limitations on the micromilling process required a channel width of 15 µm as a minimum.[2] However, using alternative strategies for preparing the molding tool, such as UV-LiGA, can significantly reduce this lateral dimension.[10]

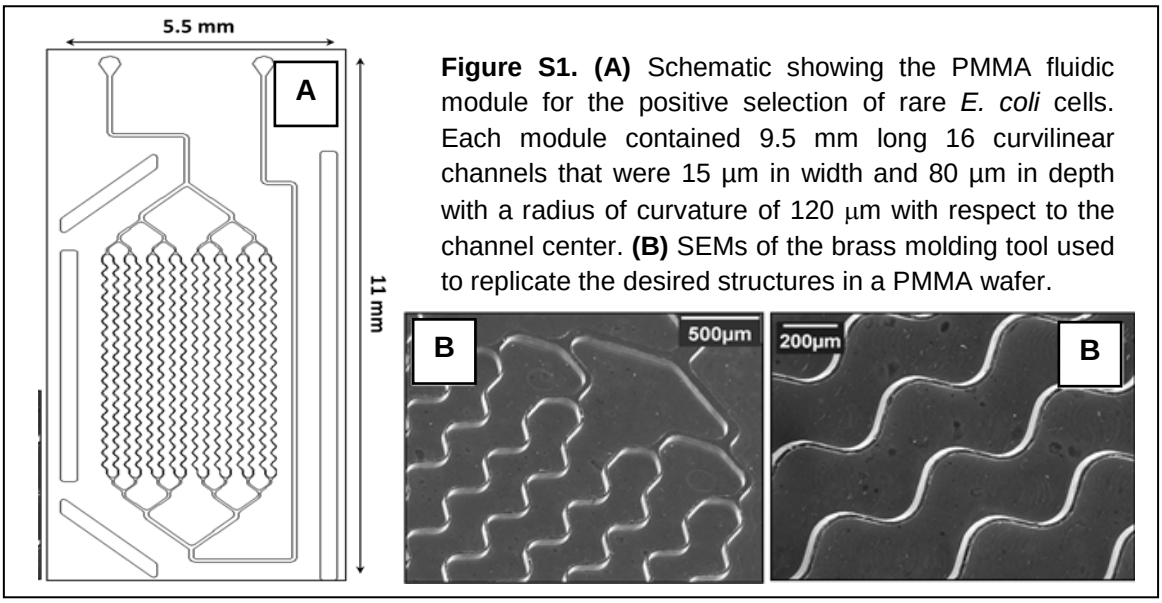

Figure S1. (A) Schematic showing the PMMA fluidic module for the positive selection of rare *E. coli* cells. Each module contained 9.5 mm long 16 curvilinear channels that were 15 µm in width and 80 µm in depth with a radius of curvature of 120 µm with respect to the channel center. **(B)** SEMs of the brass molding tool used to replicate the desired structures in a PMMA wafer.

Surface modification of PMMA and array preparation. Hot embossed PMMA microchannels were activated using an O_2 plasma.[4, 11, 12] Briefly, PMMA substrates were placed in a vacuum chamber for 1 min at 200 mTorr of oxygen pressure and 50 W of radio frequency using a Technics Series 8000 ion etcher (Surplus Process Equipment Corp., Santa Clara, CA).

For the universal array PMMA module following plasma irradiation, the substrates were soaked in 50 mg/mL EDC dissolved in a coupling buffer (pH 6.0) containing 5 mg/mL NHS for 10 min to form succinimidyl ester intermediates. The PMMA substrates were then rinsed with 18 MΩ nanopure water to remove excess EDC/NHS solution and dried with air. The freshly

prepared EDC/NHS PMMA substrates were then mounted onto a vacuum holder of a Perkin-Elmer Piezorray® non-contact microarraying instrument (Downers Grove, IL) through a custom made adapter. With the aid of a camera, 50 μM of 3'-amino-modified oligonucleotide probes (see Table S1 for sequences), separately dissolved in 0.2 M Na_2HPO_4/Na_3PO_4 buffer (pH 9.0), were spotted onto the bottom (waveguide back-side) of the embossed microfluidic channel. Dispensing volumes per spot were 330 ±30 pL and the size of the spots were ~150 μm in diameter. Following spotting, the PMMA substrates were incubated in a humidified chamber at room temperature for 4 h, washed with 0.1% SDS to remove any non-specifically bound oligonucleotides and finally dried with air. Following spotting, the PMMA module substrate was thermally fusion bonded to a PMMA cover plate to enclose the fluidic network.

Antibody immobilization to the cell selection walls of the PMMA enrichment module was carried out in a two-step process.[6] The UV-modified, thermally assembled module was flooded with a solution containing 4 mg mL^{-1} EDC, 6 mg mL^{-1} NHS in a 150 mM MES (pH = 6) for 1 h at room temperature to obtain the succinimidyl ester intermediate. After this incubation, the EDC/NHS solution was removed by flushing nuclease-free H_2O through the module. Then, 10 μL of 1.0 mg mL^{-1} of a polyclonal anti-*E. coli* O157 antibody solution in 150 mM PBS (pH = 7.4) was introduced into the channels and allowed to react for 4 h. The module was then rinsed with a solution of PBS (pH = 7.4) to remove any non-specifically bound anti-*E. coli* O157 antibodies.

PCR and LDR conditions. Two sets of PCR primers (see Table S1 for sequences) were used to amplify a 168-bp *uidA* gene from *E. coli* and a 250-bp *sipB/C* gene fragment from *Salmonella*.[13, 14] The PCR mixture consisted of 10 mM Tris-HCl (pH 8.3), 50 mM KCl, 1.5 mM $MgCl_2$, 200 μM dNTPs, 0.5 μg/μL ultra-pure bovine serum albumin (BSA), 0.5 μM of the *uidA* primer pairs, 0.8 μM of *sipB/C* primer pairs and 0.1 U/μL *Taq* DNA polymerase (New England Biolabs, Beverly, MA). The LDR mixture contained 20 mM Tris-HCl (pH 7.6), 25 mM KCl, 5 mM $MgCl_2$, 10 mM DTT, 1 mM NAD^+ (a cofactor for ligase enzyme), 0.1% Triton X-100, 0.5 μg/μL ultra-pure BSA, 50 nM of each discriminating primer, 100 nM of each Cy5-labeled common primer and 2 U/μL*Taq* DNA ligase (New England Biolabs, Beverly, MA).

The temperatures for the CF PCR were set at 95°C for denaturation, 60°C for annealing and 72°C for extension. As for the LDR, the temperatures were set at 95°C for denaturation and 65°C for ligation. CF PCR was performed at a volumetric flow rate of 1 μL/min, which provided a cycling rate of 44.6 s/cycle (8.8 s for denaturation, 8.8 s for annealing, 18 s for extension and 9 s for flowing the sample through a shallow channel connecting the extension to the denaturation zone), completing the 32 cycles for PCR in ~24 min. The CF LDR was operated at a volumetric flow rate of 2 μL/min producing a processing time of 4 min for 13 thermal cycles.

Table S1. Sequences of oligonucleotides used in the PCR/LDR/universal array assay

PCR product size (bp)	Oligos	Sequence (5'→3')	T_m (°C)[e]
168	O157-*uidA*-forward	TTACGTCCTGTAGAAACCCCAACC	58.6
	O157-*uidA*-reverse	ATCGGCGAACTGATCGTTAAAACT	56.8
	uidA-com	p[a]CAGCGTTGGTGGGAAAGCGCG-Cy5[b]	59.2
	cZip1-*uidA*-Wt	[c]**GCTGAGGTCGATGCTGAGGTCGCA**GATCGCGA AAACTGTGGAATTGAT	70.0
	cZip5-*uidA*-Mt	[c]**GCTGTACCCGATCGCAAGGTGGTC**GATCGCGA AAACTGTGGAATTGAG	70.1
250	Sal-*sipB/C*-forward	ACAGCAAAATGCGGATGCTT	56.1
	Sal-*sipB/C*-reverse	GCGCGCTCAGTGTAGGACTC	60.4
	Sal-*sipB/C*-com	p[a]CGCTAAAGATATTCTGAATAGTATTGG-Cy5[b]	51.8
	cZip11-Sal-*sipB/C*	[c]**CGCAAGGTAGGTGCTGTACCCGCA**GACAGCTT CGCAATCCGTTAG	70.9
	Zip-code 1	TGCGACCTCAGCATCGACCTCAGC-spacer-NH_2[d]	64.9
	Zip-code 3	CAGCACCTGACCATCGATCGCAGC-spacer-NH_2[d]	64.1
	Zip-code 5	GACCACCTTGCGATCGGGTACAGC-spacer-NH_2[d]	63.7
	Zip-code 11	TGCGGGTACAGCACCTACCTTGCG-spacer-NH_2[d]	65.2

[a] p: phosphorylated.
[b] Cy5: λ_{ex} = 649 nm, λ_{em} = 670 nm.
[c] The bold sequences are complementary to the sequences of zip-code probes.
[d] spacer-NH_2: $(CH_2CH_2O)_6PO_4$-NH_2
[e] Conditions: oligonucleotide concentration was 1 μM; Na^+ concentration was 50 mM.

Peripheral support equipment packaging and instrument operation (Figure S2A). Operation of all peripherals (pumps, valves, heaters, laser and CCD camera) was achieved by an Instrument Control Unit (ICU). The ICU had an on-board microprocessor that communicated with all electronic subunits (digital-to-analog and analog-to-digital converters, CCD and stepper motor drivers, temperature monitors, etc.), which controlled their operation. It also communicated with the personal computer via a USB interface and could be programmed by the user through control software. The software allowed for control of all peripherals and was used for data collection and analysis. The software could operate in two distinct modes: (1) Service mode that allowed for operator control of all hardware components individually; and (2) fully automatic mode, where all processing steps were performed according to predefined sequences without requiring any user intervention.

Two stepper-motor driven piston micro-pumps (LPVX0502600BC, Lee Company, USA) with a step resolution of 50 nL were used as positive displacement pumps (see Figure S2B). A DC motor driven mini-pump (W309-011, Hargraves Technology Corp., USA) was used for operations requiring vacuum. All inputs to the fluidic cartridge were controlled by commercial solenoid micro-valves. Pumps and valves were interfaced to the fluidic cartridge through a fluid

distribution board (FDB). The FDB was fabricated in PMMA by direct milling as were the seats for mounting the solenoid valves (6604A0-140466, Christian Bürkert GmbH & Co. KG, Germany). The connections between the FDB and fluidic cartridge consisted of standardized screw-type ferrule fluidic connectors and stainless steel tubing interconnects (see Figure S2A).

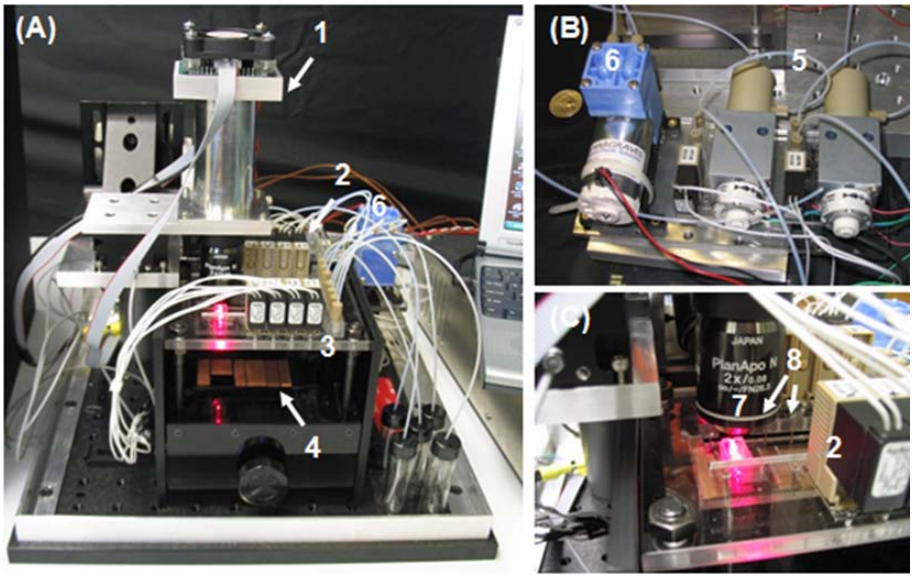

Figure S2. Photograph of the control instrument and support peripherals. (A) Fluidic cartridge peripherals: 1 – collection optics, 2 – solenoid valves, 3 – FDB and 4 – Cu heating blocks. (B) Close-up view of the fluidic elements: 5 – stepper-motor driven micro-pumps and 6 – mini-vacuum pump. (C) Close-up picture of the FDB and optical reader: 7 – imaging objective and 8 – FDB-to-chip interconnects. The instrument included an ICU, actuators, pumps, solenoid valves, heating stage, solution reservoirs and optical reader. Once the fluidic cartridge was loaded, it was aligned with respect to the FDB using stainless steel interconnects and pressed against them by raising the heating stage, which consisted of Cu blocks. This ensured both tight fluidic connections and proper heat transfer. Operation of all fluidic and electronic peripherals was achieved by the ICU.

The optical reader included an excitation laser (HL6320G, 10 mW, Hitachi), collection optics, and CCD sensor. The reader (see Figure S2C) was composed of two 2x microscope objectives (PLAPON 2x, Olympus), a 3RD660LP long pass filter and 3RD660-680 band pass filter (Omega Optics, Brattleboro, VT). The image was captured on a rectangular CCD sensor (S7030-0907; 512 x 58 pixels; 24 x 24 µm/pixel; Hamamatsu). Excitation of the array was achieved through an evanescent field produced by the waveguide serving as the floor of the microfluidic channel housing the universal array. The laser light was coupled to the waveguide via an on-chip 64° prism.[15] Both the waveguide and coupling prism were incorporated into the array module and fabricated using the same embossing step for making the fluidic network.

Commercial polyimide (KAPTON®) heaters (Minco, USA) were used to deliver heat to the PCR and LDR thermal reactors. Heaters were attached to 2 mm thick Cu blocks to achieve uniform heat flux and distribution. Temperatures were controlled by type K thermocouples

(CHAL-005, Omega Engineering, USA) placed in grooves milled into the Cu blocks. Integral to the heat management of the fluidic cartridge were thermal isolation grooves formed on the back-side of the cartridge during the embossing step, which allowed for efficient thermal isolation between adjacent reaction zones.[1] During insertion of the fluidic cartridge into the instrument, it was pressed gently against the Cu heating block surfaces covered with conductive tape to provide good thermal contact. The Cu heating blocks provided the necessary temperatures for the CF PCR and CF LDR. All pumps and valve actuators were aligned with the corresponding valves and pumps and all external fluidic connections were made through the FDB to external bulk reservoirs. This process occurred simultaneously for all elements so after a single-loading step, the system was ready for operation. All active fluidic and heating elements were under microprocessor control so that once started, the process did not require operator intervention.

The modular system was designed to perform the following processing steps: (1) Cell enrichment (optional); (2) cell lysis; (3) DNA purification; (4) ethanol wash and air dry of the SPE bed; (5) DNA release from the SPE bed with PCR buffer; (6) CF PCR; (7) mixing the PCR products with LDR buffer; (8) CF LDR; (9) DNA microarray incubation and wash; and (10) array readout and data analysis. Enriched bacterial cells were thermally lysed and suspended in an SPE immobilization buffer consisting of 3% PEG, 0.5 M NaCl and 63% ethanol and then, transported through the SPE bed. The SPE bed was washed with 85% ethanol to remove other cellular components and dried with air. Finally, the purified gDNA was released using 30 µL of the PCR buffer and pumped through the PCR CF thermal reactor at a flow rate of 1 µL/min.

Once the PCR was completed, 30 µL of an LDR reaction mixture was pumped through the cartridge at the appropriate volumetric flow rate. The resultant PCR amplicons were mixed with the LDR mixture via a passive Y-shaped micromixer possessing 40 µm wide and 100 µm deep inlet and outlet channels (aspect ratio = 3); the mixing ratio of PCR amplicons with the LDR mixture was 1 to 1. The resultant LDR products were directly pumped through the array module with the LDR products subjected to hybridization to surface-tethered zip-code probes. Following array wash with buffer (2x SSC, 0.1% SDS), fluorescence images of the arrays were collected using the optical reader consisting of a laser diode and CCD imaging sensor with a 12 mm x 3 mm field-of-view using an integration time of 20 s.

Supporting Results

Characterization of the waveguide module. For this module, the oligonucleotide zip-code probes were dispensed onto a plasma-activated PMMA surface using a noncontact spotting instrument, which eliminated any potential damage that could incur on the waveguide surface if using contact printing. Different methods of enclosing plastic channels to form a functional

device have been reported, including solvent assisted bonding,[16, 17] thermal bonding,[18, 19] adhesive boning,[20, 21] laser welding,[22] or surface modifications.[23-25] In this study, the PMMA module was assembled using thermal fusion bonding at 107°C for 20 min following spotting of the arrays. When PMMA is heated to near its Tg, it approaches a viscoelastic state,[26] which could potentially damage the oligonucleotide probes or make them inaccessible due to the polymer chain mobility burying the probes into the bulk substrate. Therefore, the stability of these DNA probes was evaluated to determine whether the thermal fusion bonding process would affect the integrity of the probes. We carried out experiments in which oligonucleotide probes (zip-code 1 and zip-code 3, see Table S1) were tethered to a PMMA sheet using the aforementioned protocol and then, one of the PMMA sheets was heated to 107°C for 20 min while the other was not. Complementary DNAs that were fluorescently labeled were dispensed onto both PMMA sheets and subjected to hybridization to the surface-tethered probes. The results of this evaluation are shown in Figure S3, which indicated no discernible decrease in fluorescence intensity after heat treatment indicating little if any chemical degradation of the spotted probes during thermal fusion bonding to enclose the fluidic network.

In our system, the PMMA module was poised on the CF LDR device. The hybridization of LDR products bearing zip-code complements to their surface-tethered zip-code probes is a thermally sensitive event. Due to the thermal conductivity of both plastics, heat from the CF LDR device can propagate to the hybridization chamber of the universal array PMMA module affecting the number of hybridions formed. To evaluate the effects of different temperatures on the fluorescence signals obtained following hybridization, different temperatures were tested including 40, 50 and 60°C. Experiments were performed in which complementary targets were pumped at a volumetric flow rate of 0.5 µL/min for 5 min through the hybridization chamber. The results indicated no noticeable decrease in fluorescence intensity at temperatures ranging from 40 – 60°C (data not shown); any temperature leakage from the CF LDR device to the universal array sitting atop this thermal processor would not affect the hybridization yield. This is a consequence of the fact that we are using a universal array in this system. The zip-code probes and zip-code complements appended to the LDR primers can be designed to have a relatively high T_m; we have decoupled the mutation detection step from the hybridization process relaxing the need for strict hybridization stringency.

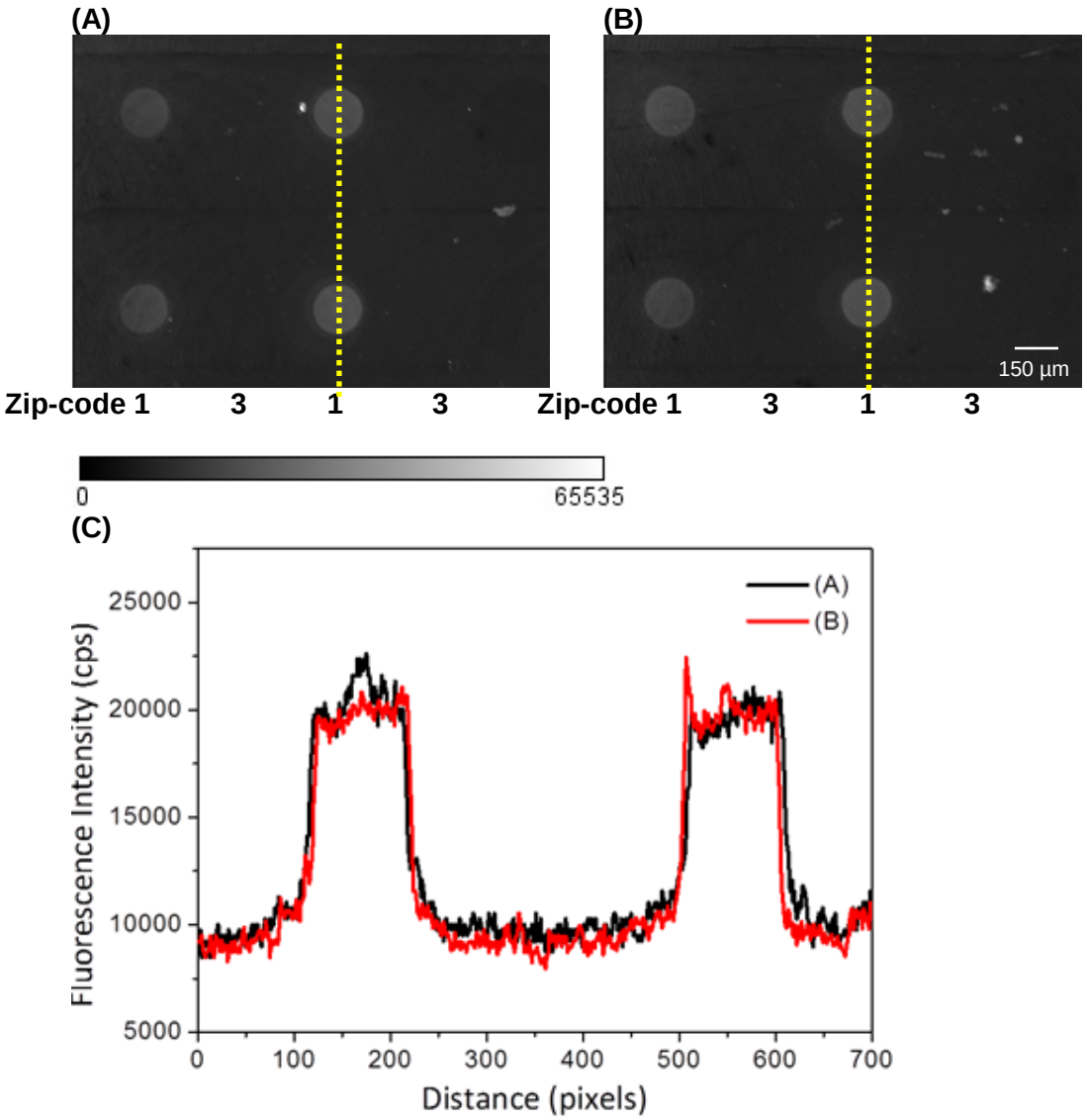

Figure S3. Effects of the thermal fusion bonding process on the stability of DNA probes. After 3'-amine-modified oligonucleotide probes (zip-code 1 and zip-code 3) were spotted onto the activated PMMA surface, PMMA sheets were either (A) heated to 107°C for 20 min or (B) not heated. The complements to zip-code probe 1 were dispensed onto both PMMA sheets followed by array hybridization, buffer wash and fluorescence imaging. The fluorescence intensity profiles from a vertical section of the middle two spots (see dotted yellow line) in (A) and (B) are shown in (C). Zip-code probe 3 served as the negative control (not a complement to the target) and zip-code 1 probed for the complementary sequence. The spot size of the universal array was ~150 µm in diameter. Each spot was done in duplicate and is represented in separate rows of the array.

Calibration curve and cell limit-of-detection. We evaluated the LOD in terms of the number of pathogenic cells we could detect with our assay and integrated system using *E. coli* O157:H7 as the target. Figure S4 presents a calibration plot of the fluorescence signal as a function of the starting *E. coli* O157:H7 cell number. The lowest cell number that produced a positive signal at a signal-to-noise ratio ≥2 was 100 cfu (colony forming units) of *E. coli* O157:H7.

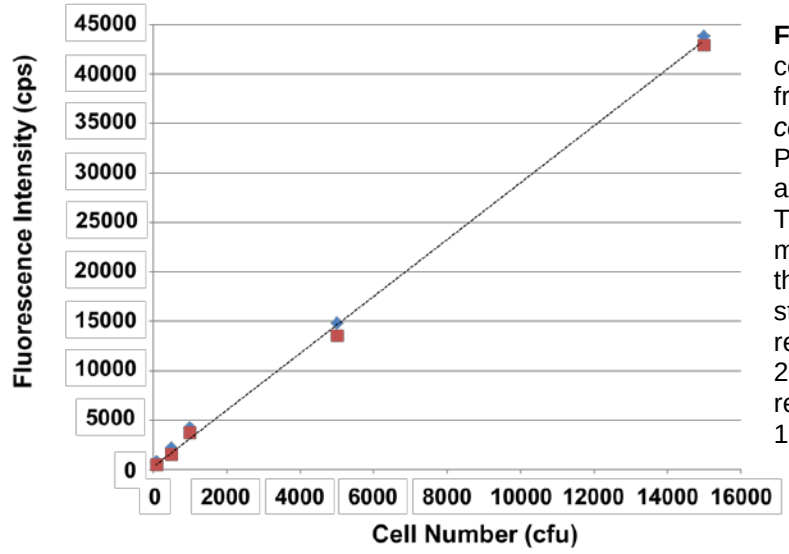

Figure S4. Standard curve consisting of fluorescence signals from various cell numbers of *E. coli* O157:H7 processed using the PCR/LDR/universal array assay and the modular fluidic cartridge. The data points represent the mean of two measurements with the error bars showing ±1 standard deviation unit. The linear regression analysis yielded: $y = 2.791x + 50.11$ ($r^2 = 0.998$). The relative standard deviations were 12%.

References

1. P. C. Chen, D. Nikitopoulos, S. A. Soper and M. C. Murphy, *Biomedical Microdevices*, 2008, **10**, 141-152.
2. M. L. Hupert, W. J. Guy, S. D. Llopis, H. Shadpour, S. Rani, D. E. Nikitopoulos and S. A. Soper, *Microfluid. Nanofluid.*, 2007, **3**, 1-11.
3. M. A. Witek, S. Llopis, A. Wheatley, R. McCarley and S. A. Soper, *Nucleic Acids Research*, 2006, **34**, e74.
4. F. Xu, P. Datta, H. Wang, S. Gurung, M. Hashimoto, S. Wei, J. Goettert, R. L. McCarley and S. A. Soper, *Anal. Chem.*, 2007, **79**, 9007-9013.
5. M. L. Hupert, W. J. Guy, S. D. Llopis, H. Shadpour, S. Rani, D. E. Nikitopoulos and S. A. Soper, *Microfluid. Nanofluid.*, 2007, **3**, 1-11.
6. A. A. Adams, P. I. Okagbare, J. Feng, M. L. Hupert, D. Patterson, J. Gottert, R. L. McCarley, D. Nikitopoulos, M. C. Murphy and S. A. Soper, *J. Am. Chem. Soc.*, 2008, **130**, 8633-8641.
7. U. Dharmasiri, S. Balamurugan, A. A. Adams, P. I. Okagbare, A. Obubuafo and S. A. Soper, *Electrophoresis*, 2009, **30**, 3289-3300.
8. U. Dharmasiri, M. A. Witek, A. A. Adams, J. K. Osiri, M. L. Hupert, T. S. Bianchi, D. L. Roelke and S. A. Soper, *Analytical Chemistry*, 2010, **82**, 2844-2849.
9. A. A. Adams, P. I. Okagbare, J. Feng, M. L. Hupert, D. Patterson, J. Gottert, R. L. McCarley, D. Nikitopoulos, M. C. Murphy and S. A. Soper, *J. Am. Chem. Soc.*, 2008, **130**, 8633-8641.
10. S. M. Ford, J. Davies, B. Kar, S. D. Qi, S. McWhorter, S. A. Soper and C. K. Malek, *J. Biomech. Eng.-Trans. ASME*, 1999, **121**, 13-21.
11. C. Situma, Y. Wang, M. Hupert, F. Barany, R. L. McCarley and S. A. Soper, *Anal. Biochem.*, 2005, **340**, 123-135.
12. S. A. Soper, M. Hashimoto, C. Situma, M. C. Murphy, R. L. McCarley, Y. W. Cheng and F. Barany, *Methods*, 2005, **37**, 103-113.
13. V. K. Sharma, E. A. Dean-Nystrom and T. A. Casey, *Molecular and Cellular Probes*, 1999, **13**, 291-302.
14. J. L. E. Ellingson, J. L. Anderson, S. A. Carlson and V. K. Sharma, *Molecular and Cellular Probes*, 2004, **18**, 51-57.
15. H. Wang, H.-W. Chen, M. L. Hupert, P.-C. Chen, P. Datta, T. L. Pittman, J. Goettert, M. C. Murphy, D. Williams, F. Barany and S. A. Soper, *Angewandte Chemie, International Edition*, 2012.
16. L. Brown, T. Koerner, J. H. Horton and R. D. Oleschuk, *Lab on a Chip*, 2006, **6**, 66-73.
17. C. H. Lin, C. H. Chao and C. W. Lan, *Sensors and Actuators B-Chemical*, 2007, **121**, 698-705.

18. Y. Sun, Y. C. Kwok and N. T. Nguyen, *Journal of Micromechanics and Microengineering*, 2006, **16**, 1681-1688.
19. X. L. Zhu, G. Liu, Y. H. Guo and Y. C. Tian, *Microsystem Technologies-Micro-and Nanosystems-Information Storage and Processing Systems*, 2007, **13**, 403-407.
20. F. J. Blanco, M. Agirregabiria, J. Garcia, J. Berganzo, M. Tijero, M. T. Arroyo, J. M. Ruano, I. Aramburu and K. Mayora, *Journal of Micromechanics and Microengineering*, 2004, **14**, 1047-1056.
21. Y. J. Pan and R. J. Yang, *Journal of Micromechanics and Microengineering*, 2006, **16**, 2666-2672.
22. T. Ussing, L. V. Petersen, C. B. Nielsen, B. Helbo and L. Hojslet, *International Journal of Advanced Manufacturing Technology*, 2007, **33**, 198-205.
23. C. W. Tsao, L. Hromada, J. Liu, P. Kumar and D. L. DeVoe, *Lab on a Chip*, 2007, **7**, 499-505.
24. M. E. Vlachopoulou, A. Tserepi, P. Pavli, P. Argitis, M. Sanopoulou and K. Misiakos, *Journal of Micromechanics and Microengineering*, 2009, **19**.
25. Y. H. Tennico, M. T. Koesdjojo, S. Kondo, D. T. Mandrell and V. T. Remcho, *Sensors and Actuators B-Chemical*, 2010, **143**, 799-804.
26. S. J. Park, K. S. Cho and C. G. Choi, *Journal of Colloid and Interface Science*, 2003, **258**, 424-426.